

Electronic Supplementary Information (ESI)

Shear-induced parallel and transverse alignments of cylinders in thin films of diblock copolymers

Yulong Chen,^{*a} Qian Xu,^a Yangfu Jin,^{*a} Xin Qian,^a Rui Ma,^a Jun Liu^{*b} and Dexin Yang^c

^a. College of Materials Science and Engineering, Zhejiang University of Technology, Hangzhou 310014, China. E-mail: chenyulong@zjut.edu.cn and jinyangfu@zjut.edu.cn

^b. Key Laboratory of Beijing City on Preparation and Processing of Novel Polymer Materials, Beijing University of Chemical Technology, Beijing 100029, China. E-mail:

liujun@mail.buct.edu.cn

^c. College of Materials & Environmental Engineering, Hangzhou Dianzi University, Hangzhou 310018, China.

Contents

Figure S1–S10

Movie S1: simulation for parallel alignment (AVI)

Movie S2: simulation for transverse alignment (AVI)

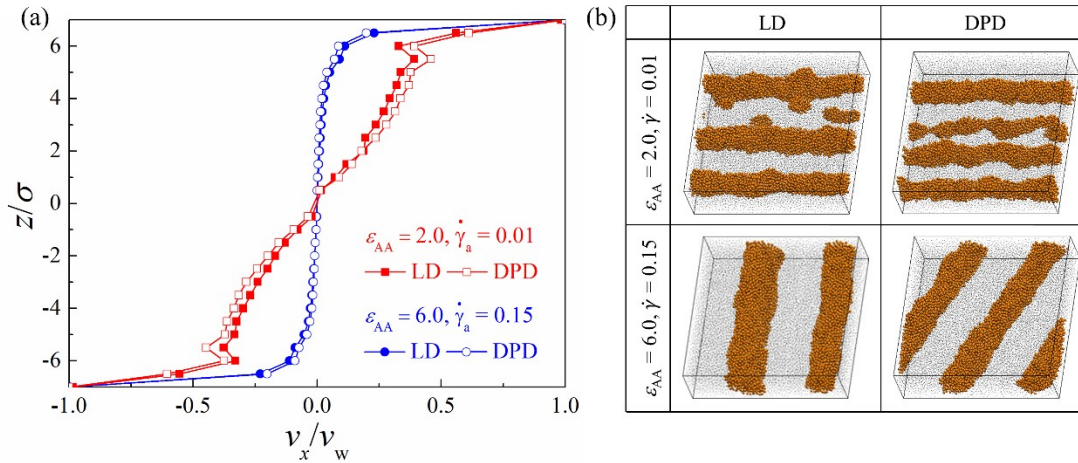


Fig. S1 Comparisons of (a) the velocity profiles along the gradient direction, normalized by wall velocity, v_x/v_w , and (b) the resulting film morphologies of shear simulations under LD and DPD thermostats. The results are shown for two typical systems at segregation strengths ϵ_{AA} and shear rates $\dot{\gamma}_a$, as indicated.

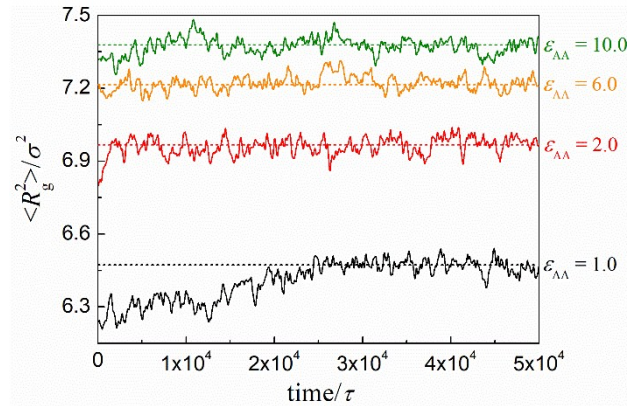


Fig. S2 Mean-squared radius of gyration $\langle R_g^2 \rangle$ of the polymer chains as a function of time for the films at various segregation strengths ϵ_{AA} as indicated.

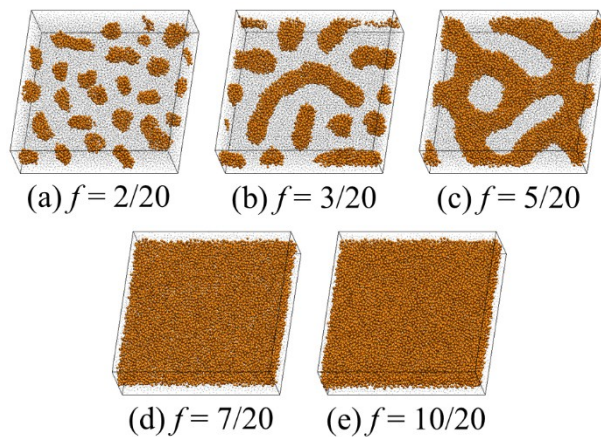


Fig. S3 Snapshots of different phases obtained by simulations: (a) spheres, (b) discrete cylinders, (c) interconnected cylinders, and (d,e) lamellae. The results are shown for the systems at the same segregation strength $\varepsilon_{AA} = 2.0\varepsilon$ but at different compositions f as indicated. The B-type beads are denoted as gray points and the confining walls are not shown for clarity.

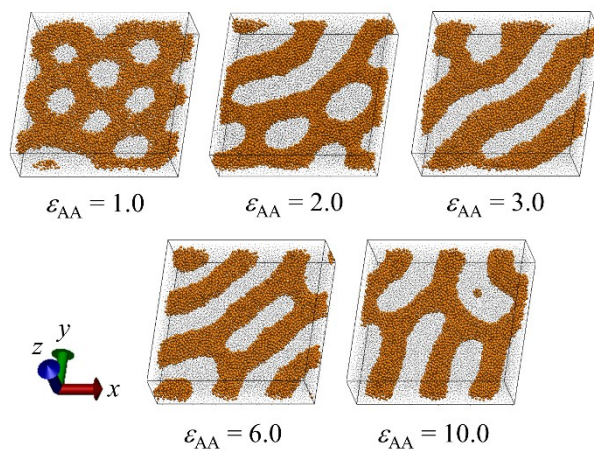


Fig. S4 Several independent simulation results presented for comparison with Fig. 2a.

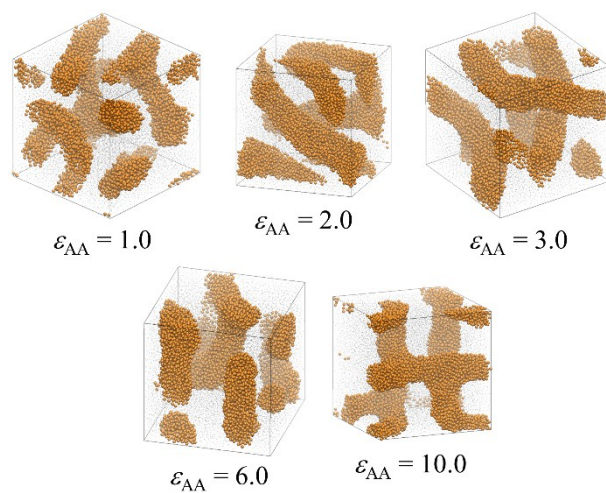


Fig. S5 Phase structures of diblock copolymers in bulk with composition $f = 5/20$ at fixed $\epsilon_{BB} = 1.0$ but at different ϵ_{AA} as indicated.

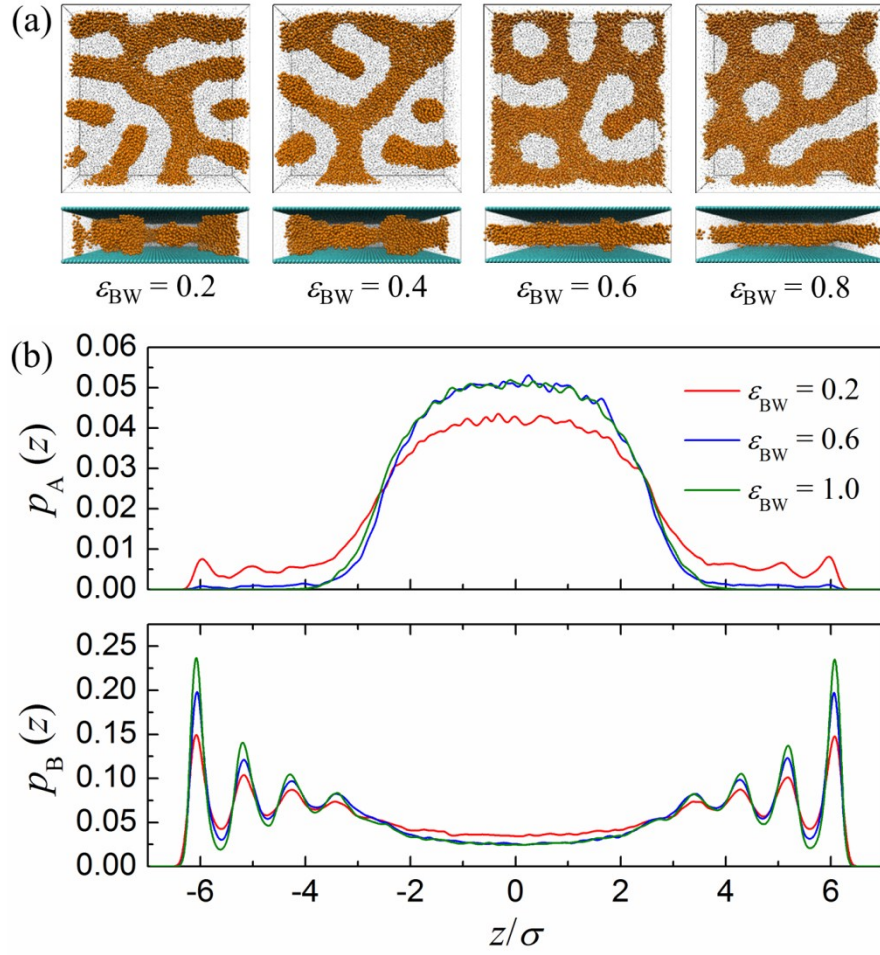


Fig. S6 (a) Top and side views of zero-shear structures of films with composition $f = 5/20$ at varying majority (B) block-wall interaction strength, ϵ_{BW} , as indicated. The confining walls in top view are rendered invisible and the B-type beads in both top and side views are denoted as gray points for clarity. (b) Density profiles as a function of height for systems at different ϵ_{BW} : top and bottom panels display the normalized probabilities of finding an A- and B-type bead at a certain point on the z -axis, $p_A(z)$ and $p_B(z)$, respectively.

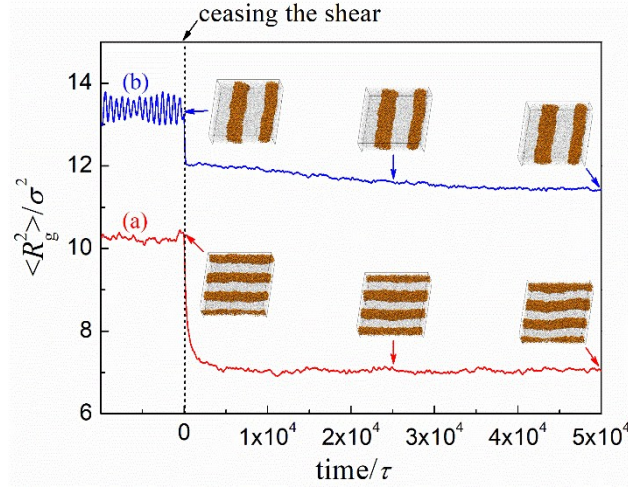


Fig. S7 Mean-squared radius of gyration $\langle R_g^2 \rangle$ of the polymer chains as a function of relaxing time for two typical systems: (a) $\varepsilon_{AA} = 2.0\varepsilon$, $\dot{\gamma}_a = 0.005\tau^{-1}$ and (b) $\varepsilon_{AA} = 6.0\varepsilon$, $\dot{\gamma}_a = 0.15\tau^{-1}$. The insets show some typical simulation snapshots where the B-type beads are denoted as gray points and the confining walls are not shown for clarity.

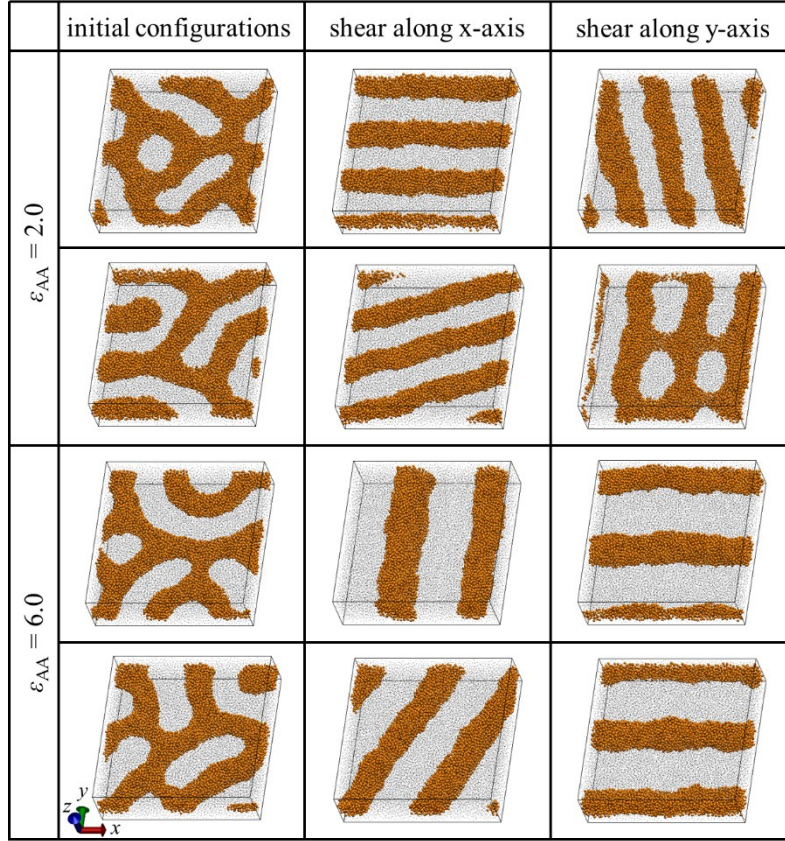


Fig. S8 Snapshots of phase structures of films at $\varepsilon_{AA} = 2.0\varepsilon$ and 6.0ε each with two different initial configurations before and after shear along both x - and y -axes at $\dot{\gamma}_a = 0.005$ and $0.15\tau^{-1}$, respectively. The B-type beads are denoted as gray points and the confining walls are not shown for clarity.

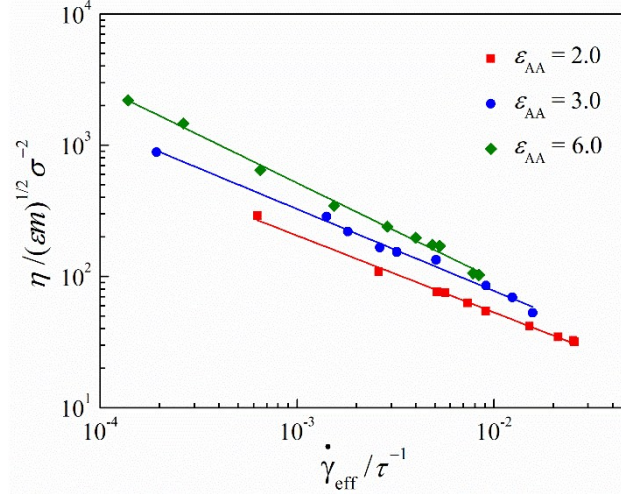


Fig. S9 Viscosity η as a function of effective shear rate $\dot{\gamma}_{eff}$ for systems of varying segregation strength as indicated. Here, the shear viscosities were calculated by $\eta = \sigma_{xz} / \dot{\gamma}_{eff}$ using only the mean value of σ_{xz} in the middle part of the film since the shear stress throughout the film is not uniform, as shown in Fig. S10.

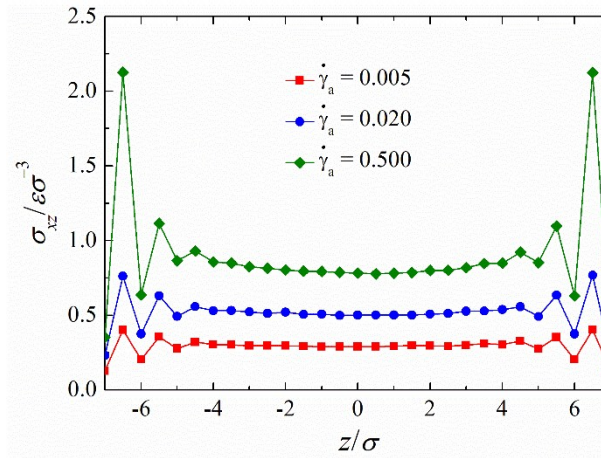


Fig. S10 Shear stress (σ_{xz}) profiles as a function of height for three typical systems at fixed segregation strength $\varepsilon_{AA} = 3.0\varepsilon$ but at varied applied shear rates $\dot{\gamma}_a$ as indicated. Here the shear stress (σ_{xz}) profiles were calculated by averaging the shear stresses of polymer beads in thin layers of width $dz = 0.5\sigma$ that are located at different distances z from the confining walls. Apparently, the shear stress throughout the film is not uniform, highly in accordance with the behavior of polymer density profiles (Fig. 2b). Although the stress profiles near the walls are oscillating, the values are almost constant in the middle of the film ($-4\sigma < z < 4\sigma$).